Inter-Active-Site Distance and Solution Dynamics of a Bivalent-Bispecific Single-Chain Antibody Molecule†

William D. Mallender,‡,§ Sergio T. Ferreira,‖ Edward W. Voss, Jr.,‡ and Tatiana Coelho-Sampaio*,‡

Department of Microbiology, University of Illinois, 131 Burrill Hall, 407 South Goodwin Avenue, Urbana, Illinois 61801, and Departamento de Bioquimica Medica, Instituto de Ciencias Biomedicas, Universidade Federal do Rio de Janeior, Rio de Janeiro, RJ 21944, Brazil

Received April 25, 1994; Revised Manuscript Received June 20, 1994®

ABSTRACT: The solution dynamics of a bivalent bispecific single-chain antibody (BiSCA) specific against fluorescein (Fl) and single-stranded DNA (ssDNA) were investigated. Fluorescence resonance energy transfer (FRET) studies were performed in order to estimate the average distances, R, between the anti-Fl and the anti-ssDNA active sites. In separate experiments, either 2-(dimethylamino)naphthalene-5-sulfonyl chloride coupled to the 5′ end of an oligothymidylate polymer of 6 residues length (2,5-DNS-dT_6) served as energy donor to Fl or eosin isothiocyanate coupled to the 5′ end of an oligothymidylate polymer of 6 residues length (eosin-dT_6) served as energy acceptor from Fl. Labeling of dT_6 with 2,5-DNS or eosin did not significantly interfere with recognition by the anti-ssDNA binding site. With the 2,5-DNS/Fl energy transfer pair, the calculated values of $R(k^2 = {}^2/_3)$, R(min), and R(max) were 44, 37, and 54 Å, respectively. With Fl/eosin (opposite direction of FRET), values of 40, 33, and 51 Å, respectively, were obtained. Considering the sizes of the two SCA domains and the length of the interdomain polypeptide linker, an R value of approximately 140 Å would be expected for the extended molecule. The fact that measured R distances were on average 3-fold shorter than 140 Å indicated that BiSCA was not an extended and rigid molecule. The efficiency of energy transfer increased with increasing temperature in the range of 10–30 °C, suggesting that conformational fluctuations of the protein resulted in decreased average distance between BiSCA active sites. The decay of the intrinsic fluorescence anisotropy in BiSCA was dominated by local mobility of tryptophan residues, as indicated by the predominance of a subnanosecond rotational correlation time component. A second rotational correlation time of approximately 7 ns was also found. The expected value for the overall rotation of the 57-kDa BiSCA molecule is approximately 21 ns. Comparison between measured and expected rotational correlation times indicated that the fluorescence anisotropy decay in BiSCA did not report overall tumbling of the whole molecule but independent rotational motions of the two SCA domains. These results, along with FRET data, suggest that BiSCA displays considerable conformational dynamics in solution, which likely results from flexibility of the linker.

Single-chain antibody (SCA)[1] molecules represent a significant innovation in the field of recombinant antibody technology (Bird et al., 1988; Huston et al., 1991). SCA molecules, consisting of the antibody variable heavy and light chain domains covalently conjugated through a polypeptide linker, retain the capacity to bind antigen (Bird et al., 1988; Ward et al., 1989; Denzin et al., 1991), but compared to intact antibodies, they possess reduced structural stability as demonstrated through *in vivo* (Yokota et al., 1992) and *in vitro* studies (Coelho-Sampaio & Voss, 1993). In order to endow SCA with bispecificity, a bivalent bispecific single-chain antibody (BiSCA) was constructed (Mallender & Voss, 1994). This molecule consists of the high-affinity anti-fluorescein SCA 4-4-20 (Bedzyk et al., 1990) and the anti-ssDNA autoantibody SCA 04-01 (Rumbley et al., 1993), covalently joined through a 24 amino acid linker as a single genetic construct. BiSCA simultaneously and independently binds fluorescein and ssDNA and possesses near wild-type affinity for the two ligands (K_d values of 3.2×10^{-10} M and 3.2×10^6 M for fluorescein and dT_6, respectively) (Mallender & Voss, 1994). Since BiSCA molecules can be expected to prove useful in biotechnological applications as well as in further understanding of antibody structure–function relationships, an examination of its structural properties in solution is mandatory. In this work, active-site orientations and dynamic conformational fluctuations exhibited by the BiSCA

† This work was supported by a grant from the Biotechnology Research Development Corp., Peoria, IL. Fluorescence measurements were performed at the Laboratory for Fluorescence Dynamics (LFD) at the University of Illinois at Urbana–Champaign (UIUC). The LFD is supported jointly by the Division of Research Resources of the National Institutes of Health (RR03155-01) and the UIUC. S.T.F. is a Pew Charitable Trusts Fellow in the Biomedical Sciences.

* To whom correspondence should be addressed.

‡ University of Illinois.

§ Supported by a National Institutes of Health Cell and Molecular Biology Training Grant.

‖ Universidade Federal do Rio de Janiero.

® Abstract published in *Advance ACS Abstracts,* August 1, 1994.

[1] Abbreviations: AEDANS, 5-[[[(2-iodoacetyl)amino]ethyl]amino]-naphthalene-1-sulfonic acid; 2,5-DNS, 2-(dimethylamino)naphthalene-5-sulfonyl chloride; BiSCA, bivalent-bispecific single-chain antibody; DNS-dT_6, 2-(dimethylamino)naphthalene-5-sulfonyl chloride coupled to the 5′ end of an oligothymidylate polymer of 6 residues length; eosin-dT_6, eosin isothiocyanate coupled to the 5′ end of an oligothymidylate polymer of 6 residues length; $F(Ab')_2$, antibody fragment containing two variable and first constant domains of the heavy and light chain (Fab domains) joined via disulfide bridges; Fab, fragment of antibody containing the variable and first constant domain of the heavy and light chain; Fl, fluorescein; FRET, fluorescence resonance energy transfer; K_d, dissociation constant for ligand dissociation from an antibody active site; Mab, monoclonal antibody; NMR, nuclear magnetic resonance spectroscopy; NZB/NZW, New Zealand black/New Zealand white inbred murine strain; PBS, phosphate-buffered saline; PEG, poly(ethylene glycol); poly(dA), polymeric single-stranded deoxyadenylate; SCA, single-chain antibody consisting of the variable heavy and variable light chains joined by an amino acid linker, ssDNA, single-stranded DNA.

0006-2960/94/0433-10100$04.50/0

molecule are studied by combining (1) measurements of fluorescence resonance energy transfer between probes bound to the two BiSCA antigen binding sites and (2) direct measurements of the rotational mobility of tryptophan residues in BiSCA.

Fluorescence resonance energy transfer (FRET) methodology [Förster, 1948; for reviews, see Stryer (1978), Stryer et al. (1982), and Cheung (1991)] is uniquely suited for determining distances between two fluorescent probes (Lakowicz, 1983). With favorable spectral overlap between the donor emission and acceptor excitation spectra, along with a relatively high donor quantum yield, energy transfer can occur over relatively large distances (10–90 Å). Both steady-state and time-resolved FRET have been used to measure distances between specific sites in proteins (Haran et al., 1992; Murase et al., 1993), phospholipid membranes (Fung & Stryer, 1978), membrane–protein systems (Corbalan-Garcia et al., 1993), and nucleic acids (Cooper & Hagerman, 1990). In particular, FRET has previously been used to examine the inter-active-site distance and Fab angle of separation in hybrid IgG molecules (Werner et al., 1972). Studies of this nature are ideal for structural analysis of the BiSCA molecule because of the high affinity, anti-fluorescein specificity of the 4-4-20 site and feasibility of labeling the dT_6 ligand (the highest affinity ligand for the 04-01 site) through a 5′ spacer with various fluorescent probes.

In this report, FRET experiments were performed in the BiSCA construct using two directions of transfer. First, 2,5-DNS-5′dT_6 was used as energy donor to the bound Fl acceptor; and second, bound Fl was the energy donor to eosin-5′dT_6. The combined results from these measurements yielded an inter-active-site distance for BiSCA which was significantly shorter (~30–35%) than predicted for an extended conformation of the molecule. In addition, measurements of the anisotropy decay of the intrinsic tryptophan fluorescence of BiSCA were carried out in order to directly assess mobility of the tryptophan residues contained in each SCA domain. By measuring fluorescence anisotropy decay, it is generally possible to resolve rotational correlation times corresponding to local mobility of the fluorophores from the overall rotation of whole protein molecules (Munro et al., 1977; Weber, 1977; Gratton et al., 1986; Ferreira, 1989; Ferreira et al., 1994). Fluorescence anisotropy decay measurements suggested that the two SCA domains in BiSCA moved independently of each other in solution. This result along with the inter-active-site distance determined from energy transfer measurements indicated that BiSCA displays considerable conformational flexibility in solution.

MATERIALS AND METHODS

Monoclonal Antibodies. Mab 4-4-20 was generated by PEG-mediated fusion of Balb/cV hyperimmune splenocytes with nonsecreting Sp2/0-Ag14 myeloma cells as previously described (Kranz & Voss, 1981). Mab 4-4-20 has been extensively characterized with an affinity for fluorescein of 1.7×10^{10} M^{-1} (Kranz & Voss, 1981; Bates et al., 1985; Herron et al., 1991). Mab 04-01 was generated by chemically mediated cell fusion of autoimmune NZB/NZW F_1 splenocytes with Sp2/0-Ag14 myeloma cells as described (Ballard et al., 1984). Mab 04-01 has been previously characterized and exhibits an affinity for oligothymidylate of 10^7 M^{-1} (Herron et al., 1989; Rumbley et al., 1993; Tetin et al., 1993).

Single-Chain Antibodies. Large-scale expression and purification of the 4-4-20 or 04-01 single-chain antibodies containing the 212 linker were carried out as previously described (Bird et al., 1988; Denzin et al., 1991; Rumbley et al., 1993).

Bivalent Bispecific Single-Chain Antibody. BiSCA was expressed in *Escherichia coli* (Mallender & Voss, 1994) and solubilized in denatured form as previously described for anti-fluorescein (Denzin et al., 1991) and auto-anti-ssDNA SCAs (Rumbley et al., 1993). Denatured BiSCA was refolded using two different methods. In one approach, BiSCA was refolded using rapid dilution followed by concentration as described (Denzin et al., 1991; Rumbley et al., 1993). Alternatively, denatured protein was refolded using a method involving dialysis against arginine-containing buffers (Kurucz et al., 1993). Briefly, denatured protein obtained from inclusion bodies was extensively dialyzed against 0.4 M arginine hydrochloride, 0.1 M Tris, pH 8.0, and 4 mM EDTA at 4 °C. The arginine refolding buffer was removed by dialysis against phosphate-buffered saline (PBS; 150 mM NaCl and 50 mM potassium phosphate, pH 8.0). Precipitate formed during the dialysis was removed by centrifugation (12 500 rpm for 30 min). Refolded BiSCA was purified using Fl–Sepharose affinity chromatography followed by ssDNA–agarose (Gibco BRL, Inc.) affinity chromatography to ensure fully active, bivalent molecules (Mallender & Voss, 1994). SDS–polyacrylamide gel electrophoresis using a 10% gel in a discontinuous SDS buffer system (Laemmli, 1970) was used to confirm purity and integrity of the 57-kDa BiSCA molecule. Protein bands were visualized with Fast Stain (Zoion Research, Inc.).

Oligodeoxynucleotide Ligands. Oligonucleotide dT_6 ligand with a 5′ free amino group was purchased from Clontech Laboratories (Palo Alto, CA). The concentration of oligonucleotide was determined using an extinction coefficient of $\epsilon_{265}^{(dT_6)} = 5.7 \times 10^4$ M^{-1} cm^{-1}. Labeling of dT_6 with 2,5-DNS (Molecular Probes, Inc. Eugene, OR) was carried out as follows: a fraction of the oligonucleotide was resuspended in 0.1 M potassium phosphate, pH 8.0, and followed by addition of K_2CO_3 (final pH of 10). 2,5-DNS (dissolved in methyl ethyl ketone) was added at a large molar excess over oligonucleotide concentration (>100-fold), and the mixture was incubated overnight at room temperature. Free 2,5-DNS was removed by chromatography on a P-2 Bio-Gel (Bio-Rad, Inc.) column equilibrated with 0.1 M potassium phosphate, pH 8. To label the dT_6 ligand with eosin, a similarly dissolved oligonucleotide sample was incubated overnight with a large molar excess (>100-fold) of eosin 5-isothiocyanate (EITC) (Molecular Probes, Inc.). Free eosin was removed by P-2 Bio-Gel chromatography as described above. DNS and eosin concentrations were determined using molar extinction coefficients of $\epsilon_{370nm} = 2090$ M^{-1} cm^{-1} and $\epsilon_{520nm} = 1.01 \times 10^5$ M^{-1} cm^{-1}, respectively.

Steady-State Fluorescence Measurements. Steady-state fluorescence data were collected on an ISS GREG PC photon-counting spectrofluorometer (ISS, Champaign, IL). Unless otherwise indicated, experiments were performed at room temperature in PBS buffer, pH 8.0. For anisotropy-based binding measurements using fluorescent labeled dT_6 ligands (Tetin et al., 1993), the concentration of the DNA ligand was kept constant at 0.1 μM and protein was titrated until saturation binding anisotropy values were reached. Studies with 2,5-DNS-modified ligand were performed using excitation at 345 m and emission observed through a KV 450 cutoff filter plus a TB400 band-pass filter. Studies with eosin-modified ligand were performed using excitation at 524 nm and emission at 553 nm. Steady-state fluorescence anisotropy data were analyzed using DeltaGraph Professional (Delta Point, Monterey, CA) as described (Tetin et al., 1993), and K_d values were determined from binding curves. For eosin-dT_6, the fraction of bound ligand correlated directly with

fluorescence anisotropy data since no changes in fluorescence intensity were observed between bound and free ligand. In the case of 2,5-DNS-dT_6, however, a 2-fold increase in fluorescence intensity was observed when a saturating concentration of either BiSCA, SCA, or Mab 04-01 was added to free 2,5-DNS-dT_6 (not shown). Differences in quantum yield between free and bound probes result in differently weighted fluorescence anisotropy values (Eftink, 1994). In order to correct for the difference in quantum yields, anisotropy data were analyzed in terms of the degree of dissociation (α) at each antibody concentration [in analogy to the procedure described by Paladini and Weber (1981)] calculated as

$$\alpha = \{1 + Q[(r - r_f)/(r_b - r)]\}^{-1} \quad (1)$$

where Q is the ratio between quantum yields of free and bound ligand, r_f is the anisotropy value for free 2,5-DNS-dT_6 (0.008), and r_b is the anisotropy for totally bound ligand (0.06).

Fluorescence Energy Transfer. In fluorescence energy transfer studies, emission spectra for DNS-dT_6/Fl (excitation at 350 nm) were recorded in the region of 370–500 nm through a TB 400-nm band-pass filter and a KV 370-nm cutoff filter. Emission spectra for Fl/eosin-dT_6 (excitation at 492 nm) were recorded in the region of 500–600 nm. Donor emission spectra were corrected for contribution from the acceptor chromophore by subtraction of the spectrum of the acceptor (in the absence of donor) and for dilution due to addition of the acceptor. Further correction for fractional occupancy of the active sites was performed as described below.

The efficiency of energy transfer from donor to acceptor (E) was calculated as

$$E = 1 - [F_{DA} - F_D(1 - f_a)]/F_D f_a \quad (2)$$

where F_{DA} and F_D are the fluorescence intensity of the donor in the presence and absence of the acceptor, respectively, and f_a is the fraction of acceptor-bound protein (Wang & Cheung, 1986). From the value of E, the average distance, R, between donor and acceptor was calculated as

$$R = R_o[(1 - E)/E]^{1/6} \quad (3)$$

The Förster critical distance (R_o) is an intrinsic constant for each energy-transfer pair, corresponding to the distance at which the efficiency of energy transfer is 50%, and was determined (Cheung, 1991) as

$$R_o = 9786 \text{ Å } (J \kappa^2 n^{-4} Q_D)^{1/6} \quad (4)$$

where κ^2 is a factor describing the relative orientation of the transition dipoles of the donor and acceptor chromophore, n is the refractive index of the medium (taken as 1.4 for aqueous medium), and Q_D is the fluorescence quantum yield of the donor in the absence of acceptor. The Q_D values used were 0.76 for 2,5-DNS (Molecular Probes) and 0.046 for antibody-bound fluorescein (Watt & Voss, 1977, 1978). J is the spectral overlap integral between the donor emission [$F(\lambda)$] and the acceptor absorption [$\epsilon(\lambda)$] spectra and can be calculated by

$$J = \int F(\lambda)\, \epsilon(\lambda)\, \lambda^4\, d\lambda / \int F(\lambda)\, d\lambda \quad (5)$$

J was calculated for the pairs 2,5-DNS/Fl and Fl/eosin by overlapping the donor emission and acceptor absorption spectra. A summation was performed at 2-nm steps for the overlapping area:

$$J = \sum I_{FD}\, \epsilon_A\, \lambda^4 / \text{area}_{FD} \quad (6)$$

Table 1: Parameters Recovered from Fluorescence Energy Transfer Measurements[a]

parameter	2,5/DNS-Fl	Fl/eosin
J	5.18×10^{-14} cm^3 M^{-1}	4.86×10^{-13} cm^3 M^{-1}
$R_{o(min)}$	35.9 Å	31.7 Å
$R_{o(max)}$	51.6 Å	48.7 Å
$R_{o(2/3)}$	42.3 Å	38.8 Å
E	0.44	0.43
$R_{(min)}$	37.4 Å	33.3 Å
$R_{(max)}$	53.7 Å	51.1 Å
$R_{(2/3)}$	44.0 Å	40.7 Å

[a] The spectral overlap integral (J) and the Förster critical distances (R_o) corresponding to the use of different κ^2 factor values were calculated as described in Materials and Methods. Experimentally determined values of energy transfer efficiency, E, were used to calculate average interprobe distances (see text).

where I_{FD} is the donor fluorescence intensity (in arbitrary units) at wavelength λ and ϵ_A is the acceptor absorption (in absorbance units) at wavelength λ of the overlapping area. Area_{FD} is the area (in fluorescence units) of the donor emission spectrum.

By determining the limiting anisotropy values for the antibody-bound probes and for the probes in 90% (w/v) sucrose solutions at −10 °C, depolarization factors for the probes were determined and utilized to calculate $\langle\kappa^2\rangle_{min}$ and $\langle\kappa^2\rangle_{max}$ [Lakey et al., 1993; reviewed in Dale et al. (1979)]. The upper and lower limits for κ^2 were calculated according to

$$\langle\kappa^2\rangle_{min} = (^2/_3)[1 - (\langle d_D^x\rangle + \langle d_A^x\rangle)/2] \quad (7)$$

$$\langle\kappa^2\rangle_{max} = (^2/_3)[1 + \langle d_D^x\rangle + \langle d_A^x\rangle + 3\langle d_D^x\rangle\langle d_A^x\rangle] \quad (8)$$

where $\langle d_D^x\rangle$ and $\langle d_A^x\rangle$ are the axial depolarization values of the attached donor and acceptor molecules, respectively. They are determined by

$$\langle d_D^x\rangle = [r_{lim(b,D)}/r_{lim(f,D)}]^{1/2} \quad (9)$$

$$\langle d_A^x\rangle = [r_{lim(b,A)}/r_{lim(f,A)}]^{1/2} \quad (10)$$

where $r_{lim(b,D)}$ and $r_{lim(b,A)}$ are the limiting anisotropies of the bound donor and acceptor, respectively, and $r_{lim(f,D)}$ and $r_{lim(f,A)}$ are the fundamental limiting anisotropies of the free donor and acceptor, respectively. Table 1 summarizes the spectral properties used in the calculation of R_o for each donor–acceptor pair.

Time-Resolved Fluorescence Measurements. Fluorescence lifetimes and dynamic polarization data were collected on a multifrequency phase and modulation fluorometer (Gratton & Linkeman, 1983). Excitation of protein tryptophan residues at 295 nm was accomplished by employing the harmonic content of a mode-locked, frequency, frequency-doubled Nd–YAG laser (Coherent Antares Model 76; Coherent, Palo Alto, CA) used to pump cavity-dumped, externally frequency-doubled rhodamine 6G dye laser (Coherent Model 700). In lifetime measurements, fluorescence emission was collected through a Schott WG 335 cutoff filter, with the excitation beam polarized to 0° and the emission observed at 55°. Color errors in photomultiplier response were minimized by using a standard solution of *p*-terphenyl (Eastman-Kodak, Rochester, NY) in cyclohexane (lifetime = 1.05 ns). Phase-modulation measurements were carried out at 12 or 13 frequencies (for fluorescence lifetime or anisotropy decay measurements, respectively) ranging from 7 to 220 MHz. Standard deviations of ±0.2° and ±0.004 were accepted for phase angles and modulation ratios, respectively. Data analysis was performed using the Globals Unlimited Software

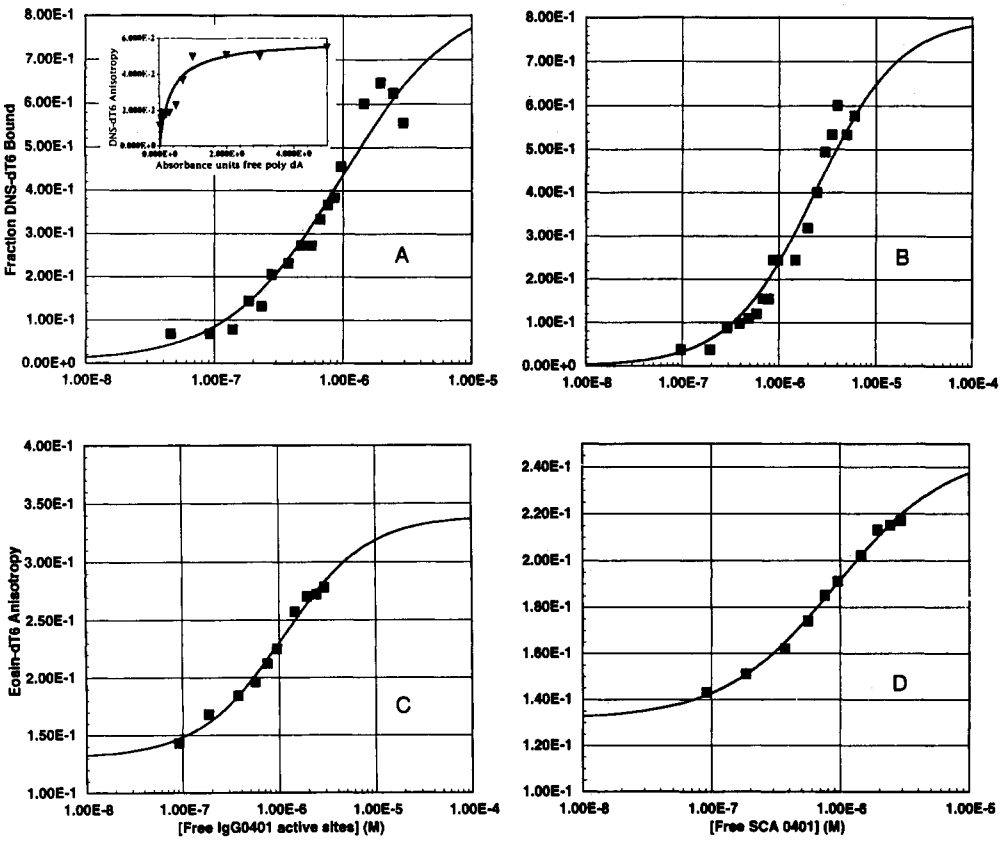

FIGURE 1: Binding of fluorescent labeled oligonucleotides to 04-01 antibodies. Binding of fluorescent oligonucleotides to anti-ssDNA antibodies was monitored by measuring increased fluorescence anisotropy of either 2,5-DNS-dT_6 (panels A and B) or eosin-dT_6 (panels C and D). Panels A and C show binding of labeled dT_6 to Mab 04-01, while panels B and D show binding to SCA 04-01. Fluorescence anisotropy measurements and curve fits were performed as described in Materials and Methods. Binding data for 2,5-DNS-dT_6 (panels A and B) was corrected and plotted as fraction bound due to the difference in quantum yield between bound and free ligand (see Materials and Methods). The inset shows binding of 2,5-DNS-dT_6 to polymers of poly(dA) averaging 360 kDa (see text).

(Laboratory for Fluorescence Dynamics, Department of Physics, University of Illinois at Urbana–Champaign, IL) (Beechem et al., 1991). Reduced χ^2 values obtained in the minimizations and the distributions of residuals were used to evaluate the goodness of fits.

RESULTS

Binding of Fluorescent Labeled dT_6 to 04-01 Antibodies. In order to test whether labeling of dT_6 with the fluorescent probes 2,5-DNS or eosin interfered with recognition by the 04-01 antibodies, fluorescence anisotropy-based binding curves were obtained using Mab and SCA 04-01 (Figure 1). Fluorescence anisotropy values of both 2,5-DNS-dT_6 and eosin-dT_6 increased with antibody concentration, indicating specific binding of the oligonucleotides to the protein. K_d values found for 2,5-DNS-dT_6 were 9.5×10^{-7} M for Mab 04-01 and 2.3×10^{-6} M for SCA 04-01. These values were in agreement with the K_d values of 1.3×10^{-7} M and 3.2×10^{-6} M, respectively, previously reported for Mab 04-01 and SCA 04-01, using tryptophan fluorescence quenching-based binding plots (Tetin et al., 1993). When eosin-dT_6 was used instead of 2,5-DNS-dT_6, the K_d values for Mab and SCA 04-01 were 1.8×10^{-6} M and 9.2×10^{-7} M, respectively. It is interesting to note that the maximal anisotropy reached using the 2,5-DNS nucleotide was close to 0.05, which was a relatively low value considering the size of the antibody molecules to which 2,5-DNS-dT_6 was bound. For this reason, the anisotropy of 2,5-DNS-dT_6 hybridized to polymers of poly(dA) averaging 350 kDa was measured (Figure 1A, inset). Again, the maximal anisotropy obtained was around 0.06, showing that a low fluorescence anisotropy characterized the 2,5-DNS-dT_6 conjugate even when associated with large molecules. This result suggested that local mobility of the 2,5-DNS group strongly contributed to the final anisotropy.

Fluorescence Resonance Energy Transfer between the Two BiSCA Antigen Binding Sites. Fluorescence resonance energy transfer measurements using BiSCA were performed using two different formats. In the first, energy transfer was assayed from the 04-01 binding site possessing bound 2,5-DNS-dT_6 to the 4-4-20 liganded (Fl) site. In the second format, the direction of energy transfer was reversed; *i.e.*, bound Fl was the donor and the eosin-dT_6 conjugate was the acceptor. The extent of transfer was quantified as quenching of donor fluorescence induced by presence of acceptor. Energy transfer was also demonstrated by increased (sensitized) fluorescence emission of the acceptor. Figure 2 shows results obtained using the 2,5-DNS/Fl pair. Addition of Fl promoted a decrease in 2,5-DNS fluorescence intensity (Figure 2A), indicating energy transfer, which was confirmed by the observation that Fl fluorescence increased upon addition of 2,5-DNS-dT_6 (Figure 2C). When BiSCA was replaced by a mixture of isolated SCAs 04-01 and 4-4-20, quenching of donor fluorescence was not observed (Figure 2B), showing that energy transfer occurred only when the two binding sites were joined in the BiSCA molecule.

The fact that the K_d of the 04-01 binding site for dT_6 was in the range of 10^{-6}–10^{-7} M prevented an experimental design in which 100% of donor was bound to BiSCA. Under the conditions used in the experiment shown in Figure 2, only 30% of 2,5-DNS-dT_6 was bound to BiSCA (based on a K_d of 2.3×10^{-6} M). Thus, the contribution of free 2,5-DNS-dT_6 had to be subtracted from the total fluorescence intensities F_D and F_{DA} used for calculation of energy-transfer efficiency (see Materials and Methods). In addition, as stated in

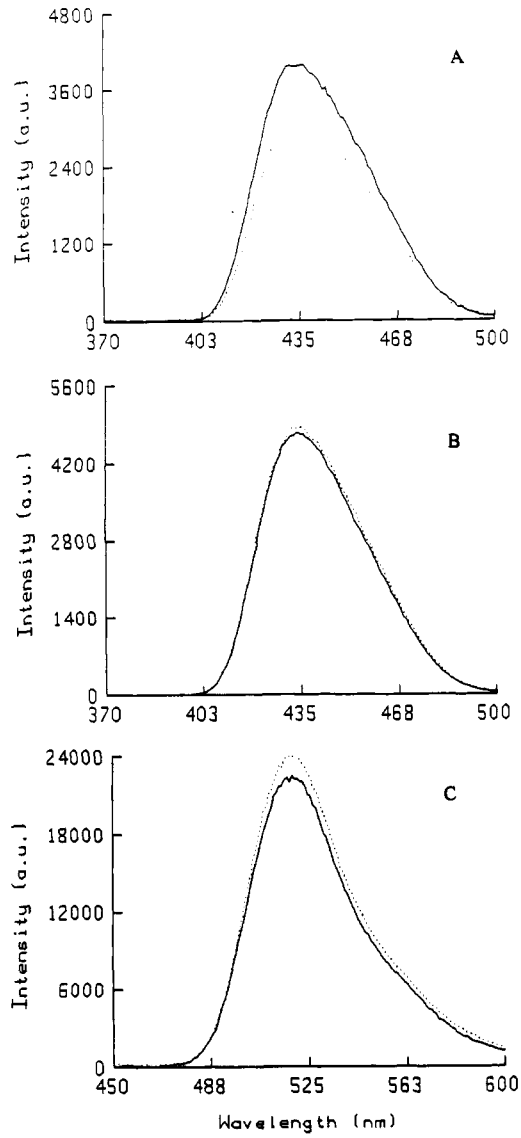

FIGURE 2: Fluorescence resonance energy transfer between 2,5-DNS-dT_6 and Fl bound to BiSCA. Fluorescence emission spectra (excitation at 345 nm) of 2,5-DNS-dT_6 in the presence of either BiSCA (panel A) or a mixture of SCA 4-4-20 plus SCA 04-01 (panel B) were measured in the absence (solid line) or in the presence of Fl (dotted line). The concentrations of antibodies, dT_6, and Fl were 1, 0.05, and 0.2 μM, respectively. In panels A and B, Fl emission was discounted by subtracting blanks where 2,5-DNS-dT_6 was omitted. Panel C shows fluorescence emission spectra of Fl bound to BiSCA in the absence (solid line) or in the presence of 2,5-DNS-dT_6 (dotted line). Spectra were corrected for 2,5-DNS-dT_6 emission.

Materials and Methods, the quantum yield of 2,5-DNS-dT_6 bound to BiSCA was twice the quantum yield of free 2,5-DNS-dT_6. In order to apply such corrections to experimentally measured fluorescence intensities, we calculated the fractional intensity corresponding to the free 2,5-DNS-dT_6 (f_{free}) as

$$f_{free} = \alpha_f Q/(\alpha_f Q + \alpha_b) \quad (11)$$

where α_f is the fraction of free dye molecules (0.70), α_b is the fraction of bound molecules (0.30), and Q is the ratio of quantum yields between free and bound 2,5-DNS-dT_6 (Q = 0.5). The fluorescence intensity corresponding to free 2,5-DNS-dT_6 (I_{free}) was then calculated as

$$I_{free} = I_T f_{free} \quad (12)$$

where I_T is the total intensity measured. Both fluorescence intensities F_D and F_{DA} were corrected by subtracting the contribution of intensity due to free 2,5-DNS-dT_6 (I_{free}).

From data corrected as explained above, the efficiency of energy transfer (E) was calculated as described in Materials and Methods. An E value of 0.44 was obtained for the 2,5-DNS/Fl pair, which, using $R_{o(2/3)}$, corresponded to an average distance of 44 Å between the two antigen binding sites in BiSCA (Table 1).

In the case of the Fl/eosin pair, the above described corrections were not necessary since the 4-4-20 binding site in BiSCA presents very high affinity for Fl (Mallender & Voss, 1994), assuring that 100% of Fl is bound to the antibody under the experimental conditions used. An E value of 0.43 was calculated on the basis of eosin-dT_6-induced quenched of Fl emission at 515 nm (not shown). The quenching of fluorescence intensity at the Fl emission peak was used instead of the integrated spectral area because the contribution of free eosin-dT_6 fluorescence (subtracted from the spectrum obtained in the presence of both Fl and eosin) was significantly high, increasing background noise in the spectrum, especially above 530 nm. The energy transfer efficiency obtained for the Fl/eosin pair corresponded to $R \sim 41$ Å [using $R_{o(2/3)}$] (Table 1). R values calculated using either energy transfer pair were significantly lower than the R distance of approximately 140 Å expected if BiSCA were an extended molecule (see Discussion). In fact, no energy transfer would be expected to occur if the distance between the two sites were of that magnitude. Thus, the observation of efficient energy transfer could have two possible interpretations. First, the polypeptide linker between the two variable domains in BiSCA could be bent, reducing the interdomain distance. An alternative explanation could be that the BiSCA molecule presented significant conformational dynamics, allowing for a wide range of motion of the two domains in solution and resulting in approximation of the two active sites. To distinguish between these two possibilities, measurements of the temperature dependence of the energy transfer as well as of the decay of fluorescence intensity and anisotropy of the tryptophan residues in BiSCA were performed, as described below.

Temperature Dependence of Energy Transfer. Fluorescence energy transfer from the 2,5-DNS-dT_6 to Fl was measured at different temperatures (Figure 3). At 10 °C no significant quenching of 2,5-DNS fluorescence was observed when Fl was added, indicating that energy transfer did not occur appreciably at this temperature. When the temperature was raised to 25 or 30 °C, fluorescence intensity was quenched by 14% or 19%, respectively (Figure 3B). Temperature limits in the experiment were set to avoid nucleotide stacking at low temperatures (<10 °C) and BiSCA denaturation at high temperatures (>30 °C). Figure 3 also shows that the decrease in 2,5-DNS fluorescence was not due to thermal quenching since fluorescence intensity of BiSCA-bound 2,5-DNS-dT_6 conjugate was unaffected by temperature in the absence of Fl (Figure 3B, open squares). Fl fluorescence, on the other hand, was quenched by about 17% upon increasing temperature from 10 to 30 °C (not shown), explaining the slight decrease in fluorescence intensity observed in the region of Fl emission with increasing temperature (Figure 3A). As an additional control, we determined that the absorption spectrum of Fl was also unaffected by temperature in the range from 10 to 30 °C (not shown), thus ruling out the possibility that the observed changes in energy transfer in this temperature range could be due to changes in the overlap integral of the 2,5-DNS-dT_6/Fl pair. The fact that energy transfer between the two BiSCA binding sites increased with temperature suggested

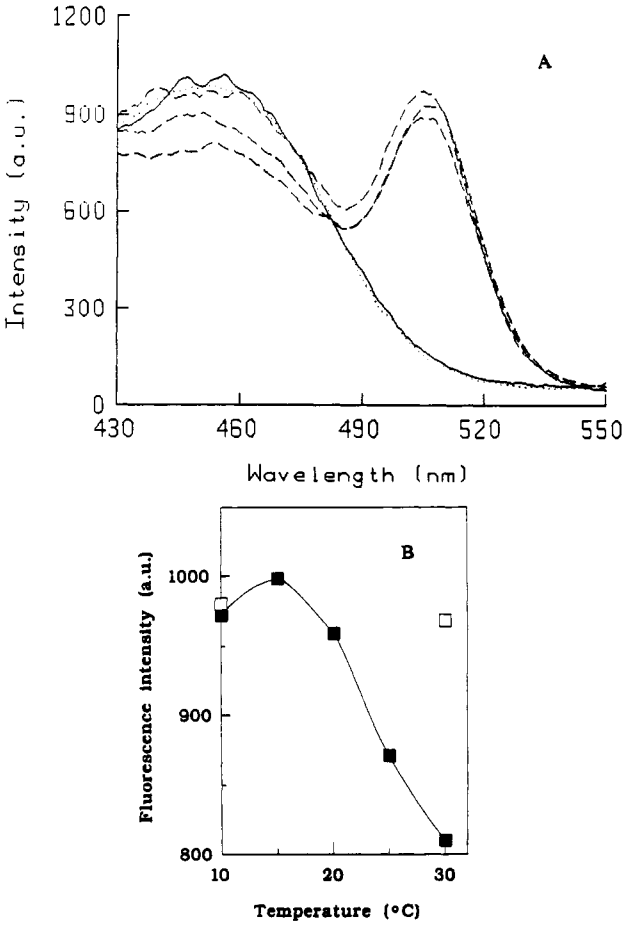

FIGURE 3: Temperature dependence of fluorescence energy transfer. Fluorescence emission spectra of 2,5-DNS-dT_6 bound to BiSCA were taken at different temperatures as indicated in panel A. Solid and dotted lines are controls done in the absence of Fl, at 10 and 30 °C, respectively. Dashed lines correspond to measurements in the presence of Fl, at 10, 25, and 30 °C (from top to bottom). Concentrations of BiSCA, 2,5-DNS-dT_6, and Fl were 1, 0.05, and 0.2 μM, respectively. Panel B shows a plot of fluorescence intensity at 455 nm (peak of 2,5-DNS-dT_6 fluorescence emission) against temperature in the absence (□) or in the presence of Fl (■).

that increased dynamics of the two SCA domains brought about an approximation of the two sites necessary for fluorescence energy transfer.

Time-Resolved Fluorescence Measurements on BiSCA, SCA 4-4-20, and SCA 04-01. Fluorescence lifteime and anisotropy decay of the tryptophan residues in BiSCA as well as in both isolated SCA 4-4-20 and 04-01 were measured with the aim to characterize these molecules in terms of structural mobility. Raw data collected in lifetime measurements (phase angles and modulation ratios) are shown in Figure 4A. Curve fits represented by the solid lines were obtained using a triple-exponential model and the parameters recovered are shown in Table 2. Attempts to analyze data using mono- or bi-exponential models produced significantly larger χ^2 values (Table 2). Data analysis employing continuous distributions of lifetime values did not result in any improvements in the fits relative to the triple-exponential model (not shown). The three SCA constructs presented two major fluorescence lifetime components at 8.5–10.7 ns and 2.7–2.8 ns. A third subnanosecond lifetime component accounted for 9–16% of the decay in the three cases.

The measured lifetime values were used in the analysis of the intrinsic fluorescence anisotropy decay of the antibodies (Figure 4B). Anisotropy decay data could not be fit to a single rotational correlation time, which yielded very high χ^2 values (Table 3). The parameters recovered using a biexponential model are shown in Table 3. For SCA 4-4-20, the two rotation correlation times found were 9.3 and 0.3 ns. These two components probably correspond to overall rotation of SCA 4-4-20 and to local mobility of the fluorophores, respectively. In fact, a rotational correlation time (ϕ) of 9.4 ns was expected for the overall rotational motion of the 26-kDa SCA 4-4-20 molecule, as calculated using

$$\phi = \eta V/RT \qquad (13)$$

where η is the viscosity of the medium, R is the gas constant, T is the absolute temperature, and V is the molecular volume, assuming a specific volume of 0.8 mL/g and an average hydration of 0.2 g of H_2O/g of protein. Similarly, two rotational components of 5.8 and 0.1 ns were found for SCA 04-01 (Table 3). The expected rotational correlation time for overall rotation of BiSCA, *i.e.*, a 57-kDa molecule, was approximately 21 ns. As shown in Table 3, the longer

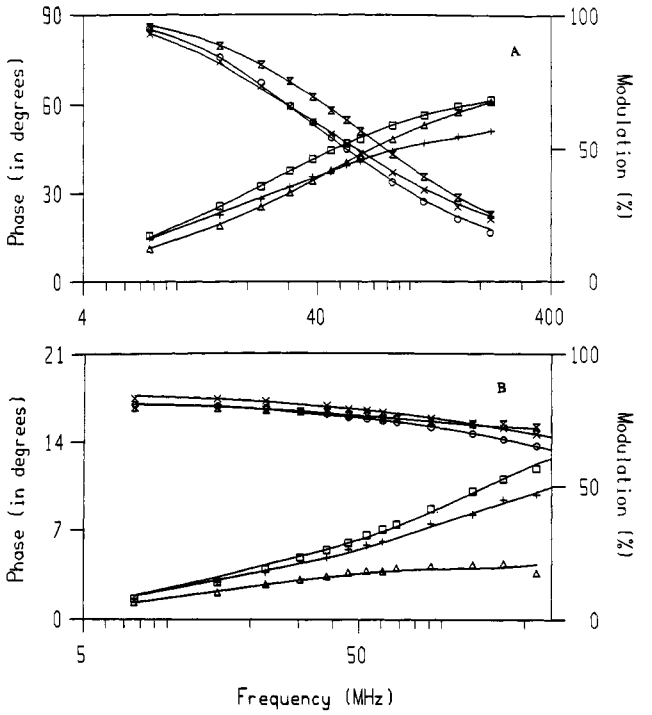

FIGURE 4: Tryptophan fluorescence decay in BiSCA, SCA 4-4-20, and SCA 04-01. Time-resolved fluorescence data were acquired using a frequency domain fluorometer as described in Materials and Methods. Lifetimes were obtained from the multifrequency phase-modulation plots shown in pane A for SCA 4-4-20, (□, ○), SCA 04-01 (△, Σ), and BiSCA (+, ×). Solid lines are nonlinear least-squares fits to the data with a sum of three exponential lifetimes (see Table 2). Panel B shows plots of the raw differential polarized phase and modulation data as a function of modulation frequency for SCA 4-4-20 (□, ○), SCA 04-01 (△, Σ) and BiSCA (+, ×). Solid lines correspond to fits using two rotational correlation times (see Table 3).

Table 2: Parameters Recovered from Lifetime Measurements[a]

parameter	SCA 4-4-20	SCA 04-01	BiSCA
χ^2 1-exponential	1421	2183	2721
χ^2 2-exponential	33.56	67.99	66.42
χ^2 3-exponential	3.057	1.450	4.094
τ_1	8.54	8.93	10.71
f_1	0.55	0.31	0.44
τ_2	2.79	2.74	2.82
f_2	0.36	0.57	0.40
τ_3	0.41	0.51	0.37
f_3	0.09	0.13	0.16

[a] Phase-modulation data were analyzed with the indicated fluorescence decay models with the Globals Unlimited software. f_i is the fractional intensity associated with τ_i in the triple-exponential fits.

Table 3: Parameters Recovered from Dynamic Polarization Measurements[a]

parameter	SCA 4-4-20	SCA 04-01	BiSCA
χ^2 1-exponential	141	101	61
χ^2 2-exponential	1.007	1.909	0.971
ϕ_1	9.34	5.83	7.34
f_1	0.22	0.32	0.16
ϕ_2	0.29	0.06	0.19
f_2	0.78	0.68	0.84

[a] Differential polarized phase/modulation data were analyzed in terms of one- or two-exponential rotational correlation times. The lifetime parameters recovered for each antibody (from the triple-exponential fits shown in Table 2) were fixed in the analysis. The limiting anisotropy, r_o, was linked in the fits for the three antibody molecules, and an r_o value of 0.32 was recovered. f_i are the fractional amplitudes corresponding to ϕ_i in the double-exponential fit.

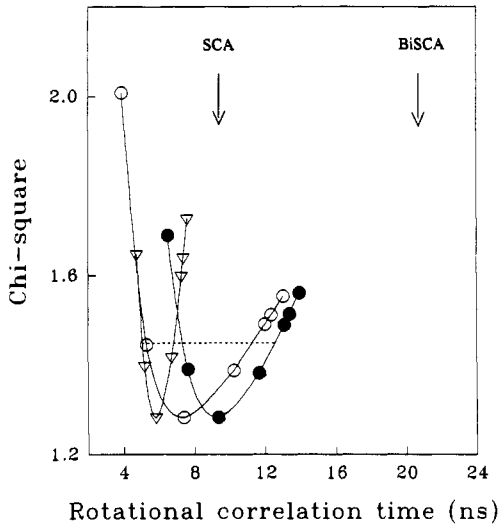

FIGURE 5: χ^2 surface analyses for the longer rotational correlation time. χ^2 surface analyses were performed to evaluate the resolvability of the longer rotational correlation times recovered for BiSCA (○), SCA 4-4-20 (●), and SCA 04-01 (△). The dashed line indicates the range of values encompassed by one standard deviation (*i.e.*, a 67% confidence interval) about the minimum. The arrows show the expected rotational correlation times for SCA and BiSCA molecules as calculated on the basis of their respective molecular weights (see Results).

rotational correlation time measured for BiSCA was 7.3 ns, about 3 times faster than the expected value. The significance of the difference between calculated and experimentally obtained rotational correlation times for BiSCA was evaluated by analyzing the χ^2 surface for this parameter (Figure 5). This analysis enables evaluation of resolvability and confidence intervals of recovered rotational correlation times (Beechem & Gratton, 1988). The fact that for BiSCA the expected rotational correlation time of 21 ns was not included in the confidence interval encompassing one standard deviation about the minimum (indicated by the dashed line in Figure 5) indicated that the longer rotation component of 7.3 ns displayed by BiSCA reports motions not associated with the overall tumbling of the whole BiSCA molecule. These motions could be associated with independent rotation of the two variable domains with respect to the polypeptide linker axis.

DISCUSSION

In this work the solution dynamics of a bivalent single-chain antibody possessing dual specificity for Fl and ssDNA was studied. The main goals were to determine the average distance between the two antigen binding sites in solution and to evaluate the dynamic motions of the two antibody domains with respect to each other. From this study valuable information was obtained regarding the conformational properties of the interdomain linker that will be useful for future design of bivalent bispecific antibodies that recognize distinct epitopes on a single macromolecule.

The K_d values obtained for binding of fluorescent labeled dT_6 to the anti-ssDNA antibodies—Mab 04-01 and SCA 04-01—showed small deviations from previously determined K_d values for the unlabeled oligonucleotide (Rumbley et al., 1993; Tetin et al., 1993). These differences were likely due to modest sterical constraints imposed by the fluorescent probe moieties in the labeled dT_6 ligand, that could prevent ideal contact between nucleotide and the binding site. In fact, analysis of the crystal structure of liganded Fab 04-01 demonstrated that the 5′ end of dT_6, where fluorescent probes are attached, makes an important contact with the binding site (Herron et al., 1989). Furthermore, antigen binding studies showed that replacement of the 5′ phosphate in dT_6 by a hydroxyl group resulted in significant loss of affinity (Tetin et al., 1993). Thus, it seems reasonable to expect the slight change in affinity observed between labeled and unlabeled oligonucleotides. It is interesting to note that the affinity of SCA 04-01 for both 2,5-DNS-dT_6 and eosin-dT_6 was actually increased when compared to the affinity for the unlabeled oligonucleotide. In contrast, affinity of Mab 04-01 was decreased in both cases. SCA molecules do not have constant domains, which makes their structure less rigid (Huston et al., 1991) and probably allows for a better accommodation of the ssDNA binding site in response to interaction with the fluorescent-labeled oligonucleotide.

The fact that fluorescence resonance energy transfer experiments in BiSCA were carried out in two directions, *i.e.*, from labeled-dT_6 to Fl and from Fl to labeled-dT_6, provided an internal control of the accuracy of the measurements. Distances calculated using either pair of probes varied by only 3–4 Å, which compared to the average R values of *ca.* 40 Å corresponds to an uncertainty of approximately 10%. Different κ^2 values were employed to evaluate the dispersion in calculated R distances that results from uncertainties in the determination of the actual dipole orientation between donor and acceptor [discussed in Dale et al. (1979)]. Minimal and maximal R distances can be calculated using $\langle\kappa^2_{min}\rangle$ and $\langle\kappa^2_{max}\rangle$, respectively, which assume relatively rigid orientations for both chromophores. In contrast, when chromophores are expected to move randomly with respect to each other, a κ^2 of $^2/_3$ is assumed. In this work, a $\kappa^2 = {}^2/_3$ was considered to be the most appropriate since steady-state fluorescence anisotropy values for antibody-bound dT_6 conjugated to either fluorescent probe were relatively low (figure 1). This result indicated that the fluorescent moieties of both dT_6 probe conjugates possessed high local mobility when complexed to the anti-ssDNA binding site, which supports the random orientation model (Haas et al., 1978). Comparison between R values calculated using the three different κ^2 factors indicated that $R_{(min)}$ and $R_{(max)}$ did not differ by more than 20% from $R_{(2/3)}$ (Table 1).

It is interesting to consider the physical interpretation for the R value measured in this work. The derivation of the Förster energy transfer equation relies on the assumption that the distance between donor and acceptor is fixed during the excited-state lifetime of the donor (Förster, 1948). In our case, significant motions on a nanosecond time scale were displayed by the two domains of BiSCA, as indicated by the anisotropy decay data (see below). Therefore, the R values recovered should be regarded as time-averaged distances between donor and acceptor. Furthermore, given the sixth power dependence of energy transfer efficiency on the distance

between the probes, the average R value will be strongly weighted by the shorter distances (Cheung, 1991).

The linker between the two single-chain antibodies in BiSCA possesses 24 amino acids. The expected length of the extended linker would be in the range of 80–90 Å, assuming a random-coil conformation as predicted by its primary sequence (Mallender & Voss, 1994). Crystal structure data reported for 04-01 and 4-4-20 Fab fragments showed that the sizes of variable domains in both cases were about 25–30 Å (Herron et al., 1989, 1991). These values are in good agreement with the recently found value of 23 Å measured through FRET analysis for the distance between bound Fl and an AEDANS probe conjugated to a Cys residue introduced by site-directed mutagenesis on the opposite side of the SCA 4-4-20 molecule (Voss and Jameson, personal communication). By adding up the linker length and the sizes for each SCA domain, a value of 140 Å is calculated for the inter-active-site distance in the extended conformation of BiSCA. This value is about 3–4 times larger than the distance measured in this work, using FRET measurements between ligands bound to each antigen binding site. In addition, the measured R distance is also lower than the size of two contiguous SCA molecules (50–60 Å). The fact that the efficiency of energy transfer between 2,5-DNS and Fl presented a definite temperature dependence (Figure 3) indicated that the smaller inter-active-site distance observed in solution resulted from dynamic motions of the BiSCA molecule. Virtually no energy transfer was observed at 10 °C, suggesting that at this temperature the average distance between the two sites approached the limit of approximately 90 Å for failure of transfer in the 2,5-DNS/Fl pair.

Measurements of dynamic polarization are frequently used to assess the rotational modes of fluorophores (Gratton et al., 1984; Lakowicz & Gryczynski, 1991). In contrast with steady-state anisotropy measurements, dynamic polarization permits the identification of distinct rotational correlation times associated with global molecular tumbling and local mobilities of fluorophores (Munro et al., 1979; Ferreira, 1989; Hazlett et al., 1989; Ferreira et al., 1994). In this work, the analysis of intrinsic dynamic polarization data for BiSCA, SCA 4-4-20, and SCA 04-01 enabled resolution of two distinct exponential rotational correlation times (Table 3). For all antibody constructs, the fluorescence anisotropy decay was dominated by local mobility of tryptophan residues, as indicated by the large fractional amplitudes corresponding to a subnanosecond rotational correlation time (Table 3). The presence of these fast rotational motions indicated that the tryptophan side chains in these proteins exhibited considerable local mobility. Despite the significant local mobility of the tryptophan side chains, the backbone of SCA may exhibit limited conformational flexibility, as demonstrated by NMR studies on an anti-phosphocholine SCA (Freund et al., 1994). The longer rotational components measured for SCA 4-4-20 and SCA 04-01 were in the range of 6–9 ns, which was in good agreement with the 9-ns value expected for the overall rotation of these molecules. For BiSCA, however, the value recovered for the longer rotational correlation time was far below the expected value. Since the rotational correlation time is directly proportional to the volume (see eq 12), an approximate doubling of the volume, in going from SCA to BiSCA, should result in a 2-fold increase in the rotational correlation time. Instead, a rotational correlation time of 7 ns was found for BiSCA. It is interesting to note that this value roughly corresponds to an average between the values obtained for SCA 4-4-20 and SCA 04-01. Anisotropy decay measurements of BiSCA at 10 °C indicated an increase in the fraction of the longer rotational correlation time (~7 ns) but still did not enable resolution of rotation corresponding to the whole 57-kDa molecule (not shown). These observations, combined with the fact that the linker does not possess tryptophan residues contributing to the intrinsic fluorescence decay, suggest that the longer rotational component in BiSCA reports independent rotational motions of the two SCA domains.

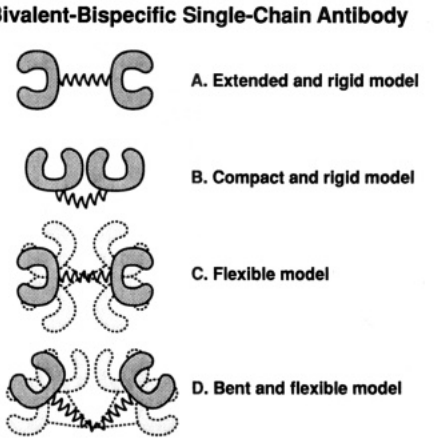

FIGURE 6: Possible models for the bivalent single-chain antibody conformation.

The expected rotational correlation times for BiSCA and for isolated SCA constructs were calculated assuming spherical shapes for these molecules (eq 12). If BiSCA had an elongated rod shape, an ellipsoid model could be more appropriate to describe its global mobility. However, if this were the case, the longer rotational correlation time measured would be larger than that calculated for a sphere (Brunet et al., 1994). The longer rotational component measured was significantly lower than the calculated value, indicating that the difference between expected and measured rotational correlation times for BiSCA was not caused by the fact that a spherical shape was assumed in calculations.

The time window through which dynamic phenomena such as the rotational diffusion of a given fluorophore can be observed by fluorescence spectroscopy depends on the lifetime of the fluorophore. Thus, the absence of a rotational component corresponding to the tumbling of the whole BiSCA molecule in our measurements could be due to the short (~4 ns) lifetime of tryptophan, which could preclude detection of such long rotational correlation times. For this reason, BiSCA was covalently labeled with the probe 2,5-DNS, which possesses a lifetime of approximately 29 ns (Herron & Voss, 1981), and dynamic polarization data were collected. Using 2,5-DNS-labeled BiSCA, two rotational components were recovered whose values were similar to those obtained using tryptophan fluorescence (data not shown). The failure of 2,5-DNS to report the overall mobility of BiSCA was probably due to fast local mobility of the probe when bound to the protein. This interpretation was supported by the low steady-state anisotropy (<0.1) found for 2,5-DNS-BiSCA (not shown). The linkers between the two variable domains in SCA have two lysine residues each (Bedzyk et al., 1990; Rumbley et al., 1993), which are probably the most easily accessible reaction sites for 2,5-DNS. Thus, in the case of 2,5-DNS-BiSCA, the strong contribution from local mobility to the anisotropy decay was probably associated with molecular flexibility of the linkers between the two variable regions in each SCA domain. In this regard, the linker region of an SCA molecule has recently been shown to exhibit substantial fast internal motion, on the basis of NMR studies (Freund et al., 1994).

In conclusion, these studies showed that BiSCA undergoes dynamic structural fluctuations in solution. This is consistent with the fact that the linker used in the BiSCA construct was a flexible peptide that permits independent motions of the two SCA domains covalently linked in this molecule. Previous studies have shown that for $F(ab')_2$ there is considerable hinge motion between the two Fab domains, which may be biologically significant in facilitating the formation of antibody–antigen complexes (Yguerabide et al., 1970). Data presented here indicate that BiSCA behaves in a similar manner. Three possible models for the conformation of BiSCA are presented in Figure 6. Our results demonstrated that BiSCA was neither an extended rigid molecule (A) nor a compact rigid molecule (B) but a flexible protein (C and/or D). The implications of this finding relate to the possibility to designing BiSCA molecules able to bind different epitopes in a single macromolecule, endowing this recombinant antibody construct with chemically defined polyclonal-like activity toward antigen.

ACKNOWLEDGMENT

We thank Cathy Rumbley for critical reading of the manuscript.

REFERENCES

Ballard, D. M., Lynn, S. P., Gardner, J. F., & Voss, E. W., Jr. (1984) *J. Biol. Chem. 259*, 3492–3498.

Bates, R. M., Ballard, D. M., & Voss, E. W., Jr. (1985) *Mol. Immunol. 22*, 871–877.

Bedzyk, W. D., Weider, K. M., Denzin, L. K., Johnson, L. S., Hardman, K. D., Pantoliano, M. W., Asel, E. D., & Voss, E. W., Jr. (1990) *J. Biol. Chem. 265*, 18615–18620.

Beechem, J. M., & Gratton, E. (1988) *Proc. SPIC—Int. Soc. Opt. Eng. (Time-resolved laser spectroscopy in biochemistry) 909*, 70–81.

Beechem, J. M., Gratton, E., Ameloot, M., Knutson, J. R., & Brand, L. (1991) in *Topics in Fluorescence Spectroscopy, Vol. 2, Principles* (Lakowicz, J. R., Ed.) pp 241–305, Plenum Publishing Co., New York.

Bird, R. E., Hardman, K. D., Jacobsen, J. W., Johnson, S., Kaufman, B. M., Lee, S.-M., Lee, T., Pope, S. H., Riordan, G. S., & Whitlow, M. (1988) *Science 242*, 423–426.

Brunet, J. E., Vargas, V., Gratton, E., & Jameson, D. M. (1994) *Biophys. J. 66*, 446–453.

Cheung, H. C. (1991) in *Topics in Fluorescence Spectroscopy, Vol. 2, Principles* (Lakowicz, J. R., Ed.) pp 128–176, Plenum Publishing Co., New York.

Coelho-Sampaio, T., & Voss, E. W., Jr. (1993) *Biochemistry 32*, 10929–10935.

Cooper, J. P., & Hagerman, P. J. (1990) *Biochemistry 29*, 9261–9268.

Corbalan-Garcia, S., Teruel, J. A., & Gomez-Gernandez, J. C. (1993) *Eur. J. Biochem. 217*, 737–744.

Dale, R. E., Eisinger, J., & Blumberg, W. E. (1979) *Biophys. J. 26*, 161–194.

Denzin, L. K., Whitlow, M., & Voss, E. W., Jr. (1991) *J. Biol. Chem. 266*, 14095–14103.

Eftink, M. R. (1994) *Biophys. J. 66*, 482–501.

Ferreira, S. T. (1989) *Biochemistry 28*, 10066–10072.

Ferreira, S. T., Stella, L., & Gratton, E. (1994) *Biophys. J. 66*, 1185–1196.

Förster, T. (1948) *Ann. Phys. 2*, 55–75.

Freund, C., Ross, A., Plückthun, A., & Holak, T. A. (1994) *Biochemistry 33*, 3296–3303.

Fung, B. K.-K., & Stryer, L. (1978) *Biochemistry 17*, 5241–5248.

Gratton, E., & Linkeman, M. (1983) *Biophys. J. 44*, 315–324.

Gratton, E., Jameson, D. M., & Hall, R. D. (1984) *Annu. Rev. Biophys. 13*, 105–124.

Gratton, E., Alcala, J. R., & Marriot, G. (1986) *Biochem. Soc. Trans. 14*, 835–838.

Haas, E., Katchalski-Katzir, E., & Steinberg, I. Z. (1978) *Biochemistry 17*, 5064–5070.

Haran, G., Haas, E., Szpikowska, B. K., & Mas, M. T. (1992) *Proc. Natl. Acad. Sci. U.S.A. 89*, 11764–11768.

Hazlett, T. L., Johnson, A. E., & Jameson, D. M. (1989) *Biochemistry 28*, 4109–4117.

Herron, J. N., & Voss, E. W., Jr. (1981) *J. Biochem. Biophys. Methods 5*, 1–17.

Herron, J. N., He, X. M., Mason, M. L., Voss, E. W., Jr., & Edmundson, A. B. (1989) *Proteins: Struct., Funct., Genet. 5*, 271–280.

Herron, J. N., He, X. M., Ballard, D. W., Blier, P. R., Pace, P. E., Bothwell, A. L. M., Voss, E. W., Jr., & Edmundson, A. B. (1991) *Proteins: Struct., Funct., Genet. 11*, 159–175.

Huston, J. S., Mudgett-Hunter, M., Tai, M., McCartney, J., Warren, F., Haber, E., & Opperman, H. (1991) *Methods Enzymol. 203*, 46–98.

Kranz, D. M., & Voss, E. W., Jr. (1981) *Mol. Immunol. 18*, 889–898.

Kurucz, I., Jost, C. R., George, A. J. T., Andrew, S. M., & Segal, D. M. (1993) *Proc. Natl. Acad. Sci. U.S.A. 90*, 3830–3834.

Laemmli, U. K. (1970) *Nature 227*, 680–685.

Lakey, J. H., Duchi, D., Gonzalez-Manñas, J.-M., Baty, D., & Pattus, F. (1993) *J. Mol. Biol. 230*, 1055–1067.

Lakowicz, J. R. (1983) *Principles of Fluorescence Spectroscopy*, Plenum Publishing Co., New York.

Lakowicz, J. R., & Gryczynski, I. (1994) in *Topics in Fluorescence Spectroscopy* (Lakowicz, J. R., Ed.) pp 293–335, Plenum Publishing Co., New York.

Mallender, W. D., & Voss, E. W., Jr. (1994) *J. Biol. Chem. 269*, 199–206.

Munro, I., Pecht, I., & Stryer, L. (1979) *Proc. Natl. Acad. Sci. U.S.A. 76*, 56–60.

Murase, S., Kawata, Y., & Yumoto, N. (1993) *Biochem. Biophys. Res. Commun. 195*, 1159–1164.

Paladini, A. A., & Weber, G. (1981) *Biochemistry 20*, 2587–2593.

Rumbley, C. A., Denzin, L. K., Yantz, L., Tetin, S. Y., & Voss, E. W., Jr. (1993) *J. Biol. Chem. 268*, 13667–13674.

Stryer, L. (1978) *Annu. Rev. Biochem. 47*, 819–846.

Stryer, L., Thomas, D. D., & Meares, C. F. (1992) *Annu. Rev. Biophys. Bioeng. 11*, 203–222.

Tetin, S. Y., Rumbley, C. A., Hazlett, T. L., & Voss, E. W., Jr. (1993) *Biochemistry 32*, 9011–9017.

Wang, C. L. A., & Cheung, H. C. (1986) *J. Mol. Biol. 191*, 509–521.

Ward, S. E., Gussow, D., Griffiths, A. D., Jones, P. T., & Winter, G. (1989) *Nature 341*, 544–546.

Watt, R. M., & Voss, E. W., Jr. (1977) *Immunochemistry 14*, 741–746.

Watt, R. M., & Voss, E. W., Jr. (1978) *Immunochemistry 15*, 875–882.

Weber, G. (1977) *J. Chem. Phys. 66*, 4081–4091.

Werner, T. C., Bunting, J. R., & Cathou, R. E. (1972) *Proc. Natl. Acad. Sci. U.S.A. 69*, 795–799.

Yguerabide, J., Epstein, H. F., & Stryer, L. (1970) *J. Mol. Biol. 51*, 573–590.

Yokota, T., Milenic, D. E., Whitlow, M., & Schlom, J. (1992) *Cancer Res. 52*, 3402–3408.